Pergamon

Geochimica et Cosmochimica Acta, Vol. 60, No. 1, pp. 31–41, 1996

0016-7037/96 $15.00 + .00

0016-7037(95)00370-3

Quantification of gas fluxes from the subcontinental mantle: The example of Laacher See, a maar lake in Germany

W. AESCHBACH-HERTIG,[1,*] R. KIPFER,[1] M. HOFER,[1] D. M. IMBODEN, R. WIELER,[2] and P. SIGNER[2]

[1] Environmental Physics, Swiss Federal Institute of Technology (ETH), Swiss Federal Institute for Environmental Science and Technology (EAWAG), CH-8600 Dübendorf, Switzerland
[2] Isotope Geology, Swiss Federal Institute of Technology (ETH), NO C61, CH-8902 Zurich, Switzerland

(*Received April* 5, 1995; *accepted in revised form September* 27, 1995)

Abstract—Vertical and horizontal distributions of helium and neon isotopes were measured in the water of Laacher See, a maar lake in the East Eifel volcanic field in Germany. Neon is in approximate atmospheric equilibrium throughout the lake, but the concentrations of both helium isotopes increase with depth and reach values of up to 10 (^{4}He) and 50 (^{3}He) times the atmospheric equilibrium concentration. The isotopic ratio of the helium excess, $R_{ex} = {}^3He_{ex}/{}^4He_{ex}$, is $(7.42 \pm 0.03)\cdot 10^{-6}$, i.e., $R_{ex}/R_a = 5.36 \pm 0.02$, where $R_a = 1.384\cdot 10^{-6}$ is the isotopic ratio in air. This indicates the presence of mantle-derived helium. Laacher See is thermally stratified during the summer. It acts as an almost perfect trap for injected gases. The helium concentration in the hypolimnion (deep water) approximately doubled from May to September 1991 yielding a mean ^{4}He-flux of $(10 \pm 2)\cdot 10^{12}$ atoms m^{-2} s^{-1}. This value is 30 times smaller than in Lake Nyos, Cameroon, but 20 times larger than in Crater Lake, USA. Release of bubbles of nearly pure CO_2 (>99%) observable in shallow waters at the eastern shore, as well as detected by divers in about 30 m depth, was identified as an important source of the helium excess in the lake. If carefully sampled by divers to avoid air contamination, the bubbles exhibit mantle influenced isotopic signatures not only for helium, but also for neon and argon ($^{20}Ne/^{22}Ne = 9.92 \pm 0.03$; $^{40}Ar/^{36}Ar = 391 \pm 4$). Based on the elemental ratios of carbon, neon, and argon to ^{3}He, the fluxes of volatiles from the mantle into Laacher See are determined as $7.4\cdot 10^7$ atoms m^{-2} s^{-1} for ^{3}He, $13\cdot 10^7$ atoms m^{-2} s^{-1} for ^{20}Ne, $26\cdot 10^7$ atoms m^{-2} s^{-1} for ^{36}Ar, and $6.4\cdot 10^{17}$ molecules m^{-2} s^{-1} for CO_2. Non-atmospheric neon was also found in the well "Wallenborn" in the West Eifel volcanic field with a $^{20}Ne/^{22}Ne$-ratio as high as 11.21 ± 0.06.

1. INTRODUCTION

Because of the distinct isotopic signatures of helium in its main global reservoirs, the atmosphere ($^3He/^4He \approx 1.4\cdot 10^{-6}$), the Earth's crust ($^3He/^4He \approx 2\cdot 10^{-8}$), and the mantle ($^3He/^4He \approx 10^{-5}$), the analysis of helium isotopes in fluids can help to identify the origin of gas fluxes from the interior of the Earth. Furthermore, accumulation of helium in natural water bodies, such as the ocean, lakes, or aquifers, offers an ideal opportunity to quantify natural helium fluxes and to assess their relevance for the atmospheric helium budget.

Helium from the Earth's mantle was first detected in the ocean (Clarke et al., 1969) where it is mainly released at mid ocean ridges and accumulated over centuries. The best available estimate of the oceanic helium flux from the mantle of (3 ± 1) ^{3}He atoms cm$_e^{-2}$ s^{-1} (per area of the Earth surface) is based on measured helium excesses in the ocean and estimated deep water renewal rates (Craig et al., 1975; Welhan and Craig, 1983).

As shown by surveys of $^3He/^4He$ ratios in continental fluids (Griesshaber et al., 1992; Oxburgh et al., 1986), the occurrence of mantle helium on continents is restricted to volcanically or tectonically active regions, especially to extension zones. Since volcanism on continents is less abundant than in the ocean it is generally assumed that the contribution of continental sources to the global mantle helium flux is small. However, up to now there have been only few studies which quantify the mass flux of helium of both mantle and crustal origin in continental areas. Most of them are based on accumulation of helium in groundwaters or lakes.

Examples of groundwater studies were presented by Torgersen and Clarke (1987), who gave a limit of the magnitude of mantle degassing through the stable continental crust of the Great Artesian Basin, Australia, and by Stute et al. (1992), who estimated the mantle helium flux in the Great Hungarian Plain, a region of active extension. Several recent investigations deal with mantle helium flux into lakes located in volcanic areas (Sano et al., 1990; Collier et al., 1991; Igarashi et al., 1992; Kipfer et al., 1994a). Provided that vertical exchange rates are known in these lakes, the helium fluxes can be calculated in the same way as done for the ocean by Craig et al. (1975). These rates vary significantly, not only from lake to lake but also for a given lake from year to year. The uncertainties of flux calculations made from helium measurements in lakes are tightly related to the knowledge of the residence time of the deep water and thus to a proper understanding of the physical processes in the particular lake.

This paper deals with the problem of determining the flux of mantle volatiles into Laacher See, a maar lake in the East Eifel volcanic field in Germany. The method involves two consecutive measurements of the lake's helium content during summer, when vertical water exchange is confined by thermal density stratification. The observed increase of the helium content, corrected for the effect of vertical mixing by turbulent

* *Present address*: Lamont-Doherty Earth Observatory of Columbia University, Palisades, NY, USA.

diffusion, is a direct measure of the helium flux into the lake. Turbulent diffusivity in the water column can be quantified by assessing the heat balance of different layers of the lake. Based on measured concentration ratios of ^{3}He with CO_2, neon, and argon, the flux of the latter volatiles can be calculated from the helium flux as well. The approach used here is straightforward and can also be applied to other lakes.

2. ANALYTICAL TECHNIQUES

The analytical techniques used in this study are briefly described in this section. More extensive descriptions are given by Kipfer et al. (1994a) and especially by Kipfer (1991) and Aeschbach-Hertig (1994).

Water samples were taken from a row boat using Niskin samplers and a hand-driven winch. The water was transferred into copper tubes immediately after recovery from the lake and tightly sealed off by closing stainless steel clamps on both ends. In the laboratory, extraction of the dissolved gas, cleaning and separating of the helium and neon fractions, and measurement of the two light noble gases was performed in a single sequence without intermediate storage of the gas. Gas samples were taken using a funnel to collect gas bubbles emerging from the lake. The gases were then transferred into copper tubes as well. Gas samples were connected via a separate entry to the same gas purification line as used for the water samples. The gas was expanded into small pipettes ($\sim$0.7 cm^3) while temperature and pressure were monitored.

The concentration and isotopic composition of helium and neon in water samples were measured simultaneously in different, noncommercial mass spectrometers. The helium mass spectrometer is designed for maximum linearity. This is achieved with a Baur-Signer ion source (Baur, 1980). Even if the helium content of the samples varies over more than one order of magnitude, no corrections are needed for possible nonlinearities. The resolution is adjustable and was kept at about 750, enough to fully separate the HD and ^{3}He peaks.

As a first step helium and neon in gas samples were analyzed as in water samples. If the isotopic neon composition did not agree within 2σ with atmospheric neon, a second gas aliquot was analysed on the counting system of the mass spectrometer that is normally used for the measurements of terrestrial helium. The machine was now especially tuned for neon to increase the precision of the isotopic ratios. In both analyses the energy of the ionizing electron beam was reduced to 40 eV to minimize the production of doubly charged ions. Therefore, correction of the neon measurement for $^{40}Ar^{2+}$ and CO_2^{2+} was negligible. In case of a double neon analysis the first measurement afforded the concentration, whereas the isotopic composition was derived from the second analysis.

For the argon measurement a separate gas aliquot was exposed to a suite of various getters to remove all reactive gas components and finally admitted for analysis to a different mass spectrometer commonly used to analyse extraterrestrial samples.

Helium and neon calibration is performed relative to an air standard. The gas amount in the aliquots of the standard is determined with an accuracy of 0.3%. To check the reproducibility of the extraction and preparation procedure, aliquots of an internal freshwater standard are analysed regularly. The average 1σ errors of the water samples from Laacher See are 0.4% for the ^{3}He/^{4}He-ratios, 0.6% for the absolute ^{4}He values, and 1.0% for the Ne values (Table 1). These values are close to the long-term mean reproducibility of the system.

The argon concentration in the gas samples was roughly calibrated against an internal pure rare gas standard and is covered by a systematic error of 10% due to some unknown volume ratios in the purification system.

Tritium concentrations in the water samples were measured according to the ^{3}He regrowth method introduced by Clarke et al. (1976). In the procedure used in our laboratory the water is transferred back into its original copper tube after degassing for the He-Ne analysis. It can be stored for years without significant leakage. Usually, after a period of 3 to 4 months the sample is degassed again to measure the newly produced ^{3}He. Based on this method the tritium concentration can be determined with a precision of about 3%.

3. LAACHER SEE

Laacher See is a small lake of nearly circular surface located in the East Eifel volcanic district of the Rhenish Massif (Fig. 1). The main volcanic activity in the Rhenish Massif occurred during the Tertiary. Quaternary volcanic activity started about 0.7 million years ago and was essentially confined to the west and east Eifel fields (Lippolt, 1983). The typical craters called maars were formed by phreatomagmatic eruptions, i.e., steam explosions due to contact of water with a magma chamber near the surface (Lorenz, 1973).

Some of these maars formed lakes, especially in the West Eifel. The largest maar lake—Laacher See—was formed in the East Eifel as a result of the most recent eruption of a huge volcano, about 11,000 years BP. This event is identified by tephra layers in the sediments of many central European lakes (Bogaard and Schmincke, 1985). Today, the lake in the Laacher See caldera has a maximum depth of 52 m and a surface area of 3.31 km^2, covering 27% of its drainage area (Fig. 1).

Laacher See can be classified as mesotrophic to eutrophic, i.e., in a state of moderate to high nutrient concentrations (Scharf and Oehms, 1992). It is holomictic, i.e., complete vertical homogenization of the water column occurs at least once a year in spring. Often there is a second overturn in late fall when the surface temperature drops to 4°C. In cold winters the lake may freeze over.

Numerous mineral springs are located in the Eifel region. Most of them are rich in dissolved CO_2-gas and many are commercially exploited (Ulrich, 1958). Discharge of CO_2-gas along the eastern shore of Laacher See has been known for many years (Schmidt-Ries, 1955; Bahrig, 1985). Rising gas bubbles can be observed at the surface at some locations near the eastern shore (see Fig. 1). Recently, gases from Laacher See and the Eifel have been analysed for their helium and CO_2 contents and isotopic composition. Griesshaber et al. (1992) found contributions of mantle helium in all groundwater and gas samples from the Rhenish Massif, the Rhine Graben, and the Black Forest, with distinct maxima in the vicinity of Laacher See and other sites of volcanism. Their results for gases from the eastern shore of Laacher See confirmed earlier measurements of Giggenbach et al. (1991). These gases consist of about 99% CO_2 and show a mantle signature in both ^{3}He/^{4}He and δ^{13}C.

Giggenbach et al. (1991) noted the remarkable parallels between Laacher See and Lake Nyos, Cameroon, where a catastrophic CO_2 release occurred in 1986. In fact, the gases in the two lakes have very similar isotopic compositions. However, the injected gases are released at a much faster rate from the annually mixing Laacher See than from the permanently stratified Lake Nyos. As shown by Kipfer et al. (1994a) for the case of Lake Van, eastern Turkey, considerable accumulation of helium can occur even if the residence time of the deep water is only on the order of one year. Therefore, in Laacher See we expected to find increasing gas concentrations during the period of thermal stratification in summer. In order to verify this hypothesis, two expeditions were organized in 1991, the first one in May, the second one in September. Water samples for the analysis of helium, neon, and tritium were taken in the deepest part of the lake (position

Table 1. Water samples from Laacher See

Sample No.	Depth [m]	Temp. [°C]	$^4He \cdot 10^8$ [cm^3STP/g]	$\Delta\,^4He$ [a] [%]	$^3He/^4He$ [10^{-6}]	$\delta\,^3He$ [b] [%]	$^{20}Ne \cdot 10^7$ [cm^3STP/g]	$\Delta\,^{20}Ne$ [a] [%]	^3H [TU]
Position: LA1, Date: 31 May 1991									
100	0	15.83	4.70 (4)	7.4 (9)	1.637 (8)	18.3 (6)	1.734 (23)	3.7 (13)	32.6 (7)
163	5	12.37	5.36 (4)	20.9 (10)	2.243 (13)	62.1 (9)	1.774 (23)	3.0 (13)	–[c]
173	10	9.60	6.63 (5)	47.7 (12)	3.217 (16)	132.4 (12)	1.787 (23)	1.1 (13)	32.3 (7)
168	15	6.26	8.99 (14)	97.1 (31)	4.281 (41)	209.3 (30)	1.849 (25)	1.1 (13)	–[c]
179	20	5.31	10.85 (9)	137 (2)	4.823 (19)	248.5 (14)	1.868 (24)	1.2 (13)	33.2 (7)
119	25	4.91	13.02 (11)	183 (2)	5.243 (23)	278.8 (17)	1.841 (24)	-0.7 (13)	33.2 (6)
131	30	4.79	13.88 (11)	202 (2)	5.378 (22)	288.6 (16)	1.873 (25)	0.9 (13)	32.5 (7)
177	35	4.55	18.08 (15)	293 (3)	5.851 (19)	322.8 (14)	–[c]	–[c]	30.0 (7)
132	40	4.34	20.60 (17)	347 (4)	6.087 (23)	339.8 (17)	1.863 (24)	-0.2 (13)	34.5 (7)
172	45	4.27	22.75 (18)	394 (4)	6.231 (26)	350.2 (19)	1.868 (24)	0.1 (13)	–[c]
114	51	4.32	–[c]	–[c]	–[c]	–[c]	–[c]	–[c]	31.3 (6)
Position: LA1, Date: 4 September 1991									
101	0	20.71	5.07 (11)	17.6 (25)	1.797 (16)	29.8 (11)	1.621 (14)	0.8 (8)	31.0 (9)
79	5	20.66	4.84 (3)	12.2 (7)	1.914 (9)	38.3 (7)	1.634 (13)	1.7 (8)	–[c]
72	10	13.47	11.05 (7)	150 (2)	4.899 (17)	254.0 (12)	1.764 (13)	3.4 (8)	34.3 (10)
46	15	7.26	13.54 (9)	198 (2)	5.313 (17)	283.9 (12)	1.861 (14)	2.9 (8)	–[c]
44	20	5.76	25.45 (16)	457 (4)	6.303 (19)	355.4 (14)	1.834 (14)	-0.2 (7)	33.4 (9)
109	25	5.26	28.69 (18)	526 (4)	6.480 (19)	368.2 (14)	–[c]	–[c]	31.1 (9)
87	30	4.92	25.43 (16)	454 (3)	6.347 (18)	358.6 (13)	1.843 (14)	-0.6 (7)	32.6 (9)
62	35	4.66	30.05 (19)	553 (4)	6.510 (24)	370.4 (18)	1.893 (15)	1.8 (8)	33.6 (5)
89	40	4.56	32.54 (21)	607 (4)	6.584 (26)	375.7 (19)	1.884 (14)	1.2 (8)	32.6 (8)
48	45	4.44	39.25 (25)	752 (5)	6.669 (17)	381.9 (13)	1.854 (14)	-0.5 (7)	31.0 (10)
102	50	4.44	44.31 (39)	862 (9)	6.814 (26)	392.3 (19)	–[c]	–[c]	32.3 (11)
110	50	4.44	44.51 (28)	867 (6)	6.786 (25)	390.3 (18)	1.861 (14)	-0.2 (8)	–[c]
Position: LA2, Date: 31 May 1991									
126	0	16.44	6.62 (5)	51.5 (12)	3.674 (18)	165.9 (13)	1.607 (21)	-3.3 (13)	32.3 (6)
134	20	5.31	22.83 (18)	398 (4)	6.212 (25)	348.9 (18)	1.850 (24)	0.2 (13)	33.2 (7)
142	28	4.84	18.76 (15)	308 (3)	5.904 (18)	326.6 (13)	1.827 (24)	-1.5 (13)	33.3 (7)
Position: LA3, Date: 4 September 1991									
61	15	7.14	14.92 (11)	229 (2)	5.543 (17)	300.5 (12)	1.860 (17)	2.7 (9)	35.0 (9)
113	20	5.56	20.33 (14)	344 (3)	6.020 (18)	334.9 (13)	1.885 (20)	2.4 (11)	36.2 (10)

Errors (one standard deviation) are quoted in parentheses referring to the last digits.
[a] Percent deviation of measured ^4He (^{20}Ne) concentration from solubility equilibrium by Weiss (1971).
[b] Percent deviation of measured $^3He/^4He$ ratio from atmospheric value ($1.384 \cdot 10^{-6}$, Clarke et al., 1976).
[c] Not determined

LA1, Fig. 1) at 5 m depth intervals. Quasi-continuous CTD (conductivity, temperature, depth) profiles were recorded simultaneously to monitor the physical state of the lake. Additional water samples were taken at position LA2 (May) and LA3 (September). Position LA2 was chosen because gas bubbles rising to the surface can be observed during calm wind conditions. LA3 was selected as a location far away from the supposed degassing centres to search for possible horizontal gradients.

Two samples of gas bubbling through shallow water (about 30 cm deep) were collected at the eastern shore (LA4). During a third expedition in fall 1993, divers located a major gas source in Laacher See at a depth of 31 m (LA2). They were able to take a gas sample directly at the source, i.e., before the gases came into contact with air or with atmospheric gases dissolved in the water. The data from the water samples are used to quantify the helium flux at Laacher See, whereas information on elemental ratios gained from the gas samples serves to calculate fluxes of other volatiles from this helium flux.

4. RESULTS AND DISCUSSION

4.1. Data from the Water Column of Laacher See

Vertical temperature profiles from 1991 are shown in Fig. 2. A distinct thermocline is visible between about 8 and 15 m depth, especially in September. It divides the lake into a well-mixed surface layer (epilimnion) and a vertically stratified deep-water volume (hypolimnion). The temperature scale in the inset of Fig. 2 is greatly enlarged to demonstrate the slight warming that occurred in the deepest part of the lake during summer. The warming is mostly due to turbulent diffusive heat flux from the surface. In the deepest 5 m of the water column the vertical temperature gradients are very small and even change sign. This is probably due to the combined effect of boundary layer mixing and geothermal heat flow from below. However, the temperature profiles do not indicate an enhanced geothermal flux. In fact, Haenel (1983) reported a heat flow of 76 mW m^{-2} in Laacher See, a value which is well within the typical range for nonvolcanic lakes.

While there is nothing special about the temperature data, the helium concentrations (Table 1 and Fig. 3) are remarkable. Noble gas concentrations in lakes are usually in close equilibrium with the atmosphere, as calculated from the solubility coefficients given by Weiss (1971). This applies to neon in Laacher See (Table 1). In contrast, the helium concentrations increase strongly with depth and time. Relative deviations of measured ^4He concentrations from atmospheric equilibrium, Δ^4He, are shown in Fig. 3a. Δ^4He approximately doubled from May to September and reached a maximum value of more than 8 times atmospheric equilibrium

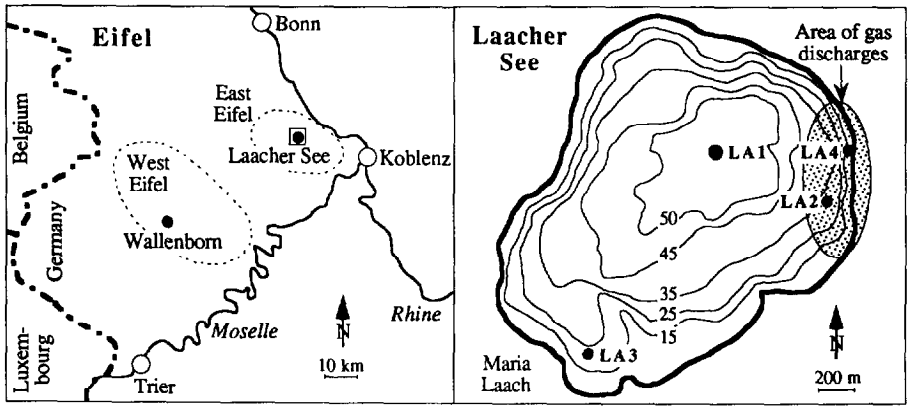

FIG. 1. Left: Map of the Eifel region showing the East and West Eifel volcanic districts and the locations discussed in the text. Right: Detailed map of Laacher See, including the sampling positions LA1 (main profiles, deepest part of the lake), LA2 (gas bubble plumes), LA3 (reference position far from sources) and LA4 (gas seepage in shallow water at the shore). Depth contours are labeled in meters.

near the bottom of the lake. The expected accumulation of helium in the lake is clearly shown by the data.

In Fig. 3a two additional features are remarkable: (1) a horizontal concentration increase from the central profile (LA1) to the eastern shore (LA2) observed in May and (2) a concentration peak around 25 m depth present at the central station in September. These observations are consistent with the existence of a strong local helium source near station LA2, where several patches of bubbles were observed at the lake surface. In fact, at one of these locations divers detected a plume of bubbles emerging from a funnel at the sediment surface at 31 m depth. The divers reported that most of the bubbles are completely dissolved within a few meters above the funnel and that only a few bubbles make it to the surface where they reveal the existence of the subsurface bubble plume. The fast dissolution of the bubbles within the water column explains the concentration maximum at 25 m depth. However, the fact that at station LA1 helium concentrations also increase below 30 m depth points to the presence of additional and deeper helium sources.

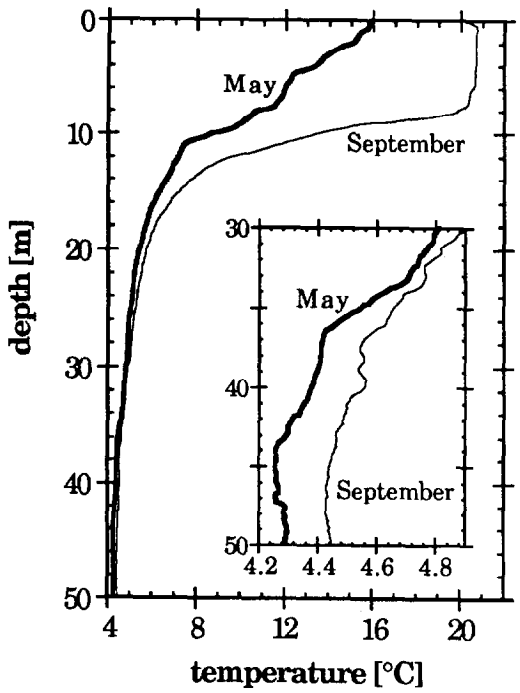

FIG. 2. Temperature profiles recorded at the central position LA1 on 31 May and 4 September 1991. Insert: Water column below 30 m with enlarged temperature scale.

As for Δ^4He, the $^3He/^4He$ ratio increases with depth and time from values close to atmospheric equilibrium at the water surface to 5 times larger values at the bottom of the lake (Fig. 3b). This indicates that the injected helium has a higher $^3He/^4He$ ratio than the atmosphere and should, at least partially, originate from the mantle. The isotope ratio of the excess component, $R_{ex} = {}^3He_{ex}/{}^4He_{ex}$, is calculated by subtracting the atmosphere-derived helium from the measured helium, using the measured neon concentrations as an indicator for the dissolved atmospheric gases (Sano et al., 1990). Only the samples from below 15 m contain sufficiently large helium excesses to allow reliable calculations. The average value obtained from these samples is $R_{ex} = (7.41 \pm 0.04) \cdot 10^{-6}$, i.e., $R_{ex}/R_a = (5.35 \pm 0.03)$, where $R_a = 1.384 \cdot 10^{-6}$ is the $^3He/^4He$ ratio in air (Clarke et al., 1976). This is in accordance with the values measured in gas samples from Laacher See by Giggenbach et al. (1991) ($R/R_a = 5.5$) and Griesshaber et al. (1992) ($R/R_a = 5.4$).

An alternative method to determine R_{ex} is based on the assumption that in each sample two components, i.e., the atmospheric component and a component of unknown origin, are present in different proportions. Thus, by plotting the observed isotope concentrations against each other (Fig. 4), a straight line should evolve which on one end passes through the point of air-saturated water (ASW). Although the other endmember cannot be located, the slope of the straight line would then correspond to the isotopic ratio of the excess component, provided that all the added helium has the same isotopic composition. This is indeed the case for all water samples from Laacher See, irrespective of the sampling date (Fig. 4). The surface samples lie near the ASW point, and the deep water samples have the highest excesses. The slope of the

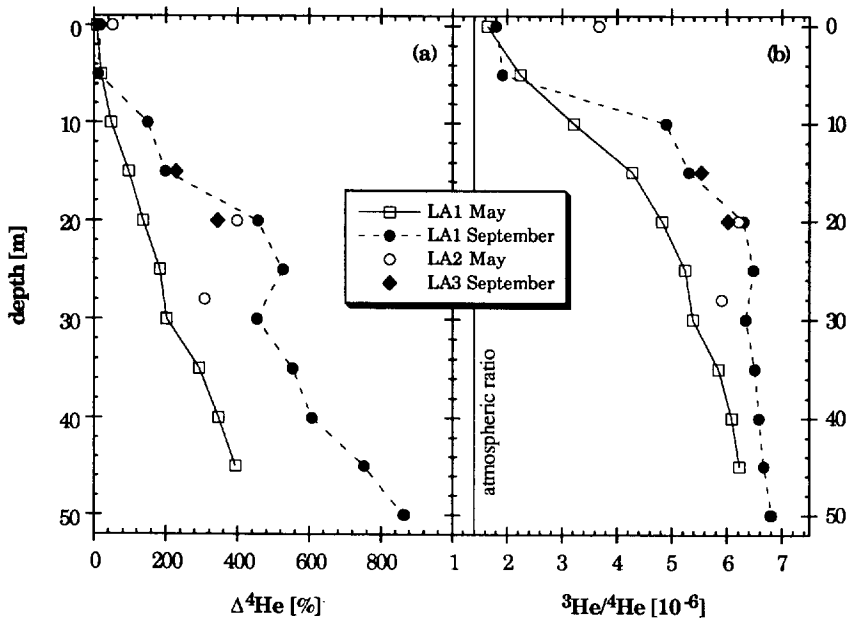

FIG. 3. Vertical profiles showing (a) Δ^4He (^{4}He excess, i.e., concentration above equilibrium with atmospheric helium, expressed in % of equilibrium concentration), (b) ^{3}He/^{4}He ratio. See Fig. 1 for location of sampling stations LA1 to LA3.

regression line is well defined giving R_{ex} = (7.42 ± 0.03)·10^{-6}, i.e., R_{ex}/R_a = (5.36 ± 0.02), in full accordance with the result derived above, but slightly more accurate.

In conclusion, two contributions to the helium measured in Laacher See can be identified: Dissolved air and excess helium injected from below. The isotopic ratio of the second contribution, R_{ex}, is lower than both typical values for the MORB mantle (≈8–9 R_a, Lupton, 1983) and ratios measured in fluid inclusions in xenoliths from the Eifel (6.03 ± 0.14) R_a (Dunai and Baur, 1995). There are different ways to explain the composition of the excess helium. Griesshaber et al. (1992) interpret it as a mixture of 68% mantle component with 8 R_a and 32% crustal component with 0.03 R_a. One could also invoke the existence of a subcontinental mantle reservoir with 6 R_a, as suggested by the results of Dunai and Baur (1995) and of Polve and Kurz (1984), and explain the deviation of the excess helium in the lake by addition of 12% crustal material. Yet, all these explanations must remain speculative, since the excellent linear correlation derived from the helium isotopes of Laacher See (Fig. 4) yields information of just two components, an atmospheric and an excess one. No doubt that the latter is ultimately the result of a two-component or even three-component mixture. But its rather constant isotopic composition suggests that the corresponding reservoir must be fairly large and stable.

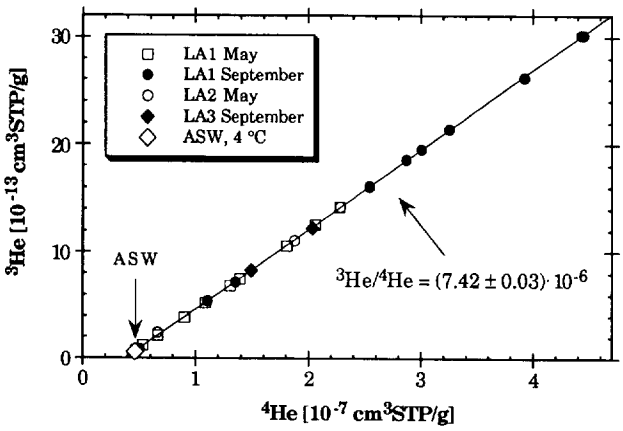

FIG. 4. Correlation of the helium isotope concentrations of all water samples from Laacher See. Surface samples plot near the point for air-saturated water (ASW), deep water samples are enriched by helium from a source with a ^{3}He/^{4}He ratio of (7.42 ± 0.03)·10^{-6}, as indicated by the slope of the regression line.

The good correlation in Fig. 4 also rules out significant contributions from tritium decay to the observed ^{3}He excess. In September, the ^{3}He excess reached nearly 300·10^{-14} cm^3 STP/g at the bottom (about 50 times the atmospheric equilibrium concentration), whereas the tritium concentration was rather constant throughout the lake at about 32 TU (1 TU corresponds to a the atomic ratio ^{3}H/^{1}H = 10^{-18}). Within one year, an upper limit for the residence time of the deep water in the lake, the β-decay of tritium would cause a ^{3}He excess of 0.4·10^{-14} cm^{3}STP/g, only about 1‰ of the observed maximum excess. Thus, in Laacher See tritiogenic ^{3}He plays only a minor role and cannot be used to calculate the ^{3}H-^{3}He water age (Torgersen et al., 1977). This deprives us of a powerful tool to quantify the residence time and the flux of helium in the lake.

Additional water and gas samples were collected from springs, wells, and three other maar lakes in the Eifel. Only the results obtained from one particular well will be discussed. The other spring samples merely confirm the findings of Griesshaber et al. (1992), whereas in the maar lakes from the West Eifel we did not find any traces of helium from the Earth's interior, neither crust nor mantle.

4.2. Noble Gas Isotopes in Gas Samples from Laacher See and Wallenborn

With the exception of helium, noble gases of non-atmospheric origin are difficult to detect, because they are often masked by atmospheric contributions. This is most likely the case in water samples from lakes, where dissolved atmospheric noble gases are always present. Non-atmospheric isotopic signatures may be found in gas samples if contamination by ambient air is carefully avoided. To estimate an upper limit of air contamination in gas samples we compare the measured concentration of the main neon isotope, ^{20}Ne, to its atmospheric abundance of 16.45 ppm.

Three gas samples from Laacher See were taken close to the shore near position LA4, where at several locations a gentle seepage of gas in knee-deep water can be observed (Table 2, No. 169, 174 and 249). In spite of the low fluxes we were able to keep air contamination small, as shown by ^{20}Ne contents in the range of 20 to 60 ppb. In contrast, helium is enriched with concentrations of 17 to 20 ppm as compared to 5.24 ppm in air. The combination of helium and neon values shows that the correction of the measured $^3He/^4He$ ratios for atmospheric helium (Griesshaber et al., 1992) is negligible (less than 1‰).

The most interesting gas sample from Laacher See is the one taken by divers at position LA2 (No. 245). By using a funnel the divers were able to collect the sample into the copper tube right at the source. In fact, air contamination was by an order of magnitude lower than in the samples from LA4. Thus, it was possible to detect small but significant deviations of the isotopic composition of neon and argon from atmospheric values (Table 2).

It is worth noting that in all gas samples from Laacher See the measured $^3He/^4He$ ratios (7.23 to $7.33 \cdot 10^{-6}$) are slightly smaller than the value calculated from the excess helium in the water samples ($(7.42 \pm 0.03) \cdot 10^{-6}$). As discussed above, the difference can neither be due to air contamination of the gas samples nor due to tritium decay in the water samples. A possible explanation is kinetic mass fractionation during dissolution of gas bubbles. Although the heavier isotope is more soluble at equilibrium conditions (Benson and Krause, 1980), it is the lighter ^3He that is exchanged faster and thus can be enriched in the water phase during the kinetic process of bubble dissolution (Fuchs et al., 1987). Kinetic fractionation was shown to alter the $\delta^{13}C$ values of CO_2 injected as gas into Laacher See (Puchelt, 1982).

The effects of gas exchange between rising gas bubbles and the surrounding water on the noble gas composition of both phases have been studied by Kennedy et al. (1988). Based on the measured partial pressures of the noble gases in the gas samples (Table 2) it is clear that in Laacher See helium is transferred from the bubbles into the water, while neon and argon will be stripped from the water into the bubbles. Quantification of these processes could be attempted by means of models such as the so-called bubble plume model which was built to describe the dynamics of artificial mixing and oxygen input as used for the restoration of eutrophic lakes (Wüest et al., 1992). This would, however, require knowledge of initial bubble radius and plume fluxes, information that is presently not available. For our discussion, application of such models is not necessary, since we are confident that the sample collected by the divers represents the original composition of the gas phase, before exchange with the lake water has taken place.

The well "Wallenborn" in the West Eifel periodically discharges gaseous CO_2 (about once an hour) causing the water surface of the well to rise. On 1 June, 1991, and 3 September, 1993, gas samples were collected during such events (Table 2, No. 30 and 68). The intense degassing makes air contamination less probable. The $^3He/^4He$ ratio of 2.66 R_a measured at Wallenborn points to a larger contribution of crustal gases than in Laacher See.

In Fig. 5, the composition of the samples from Wallenborn and Laacher See are plotted in a three-isotope diagram of neon. Both samples from Wallenborn lie close to the mixing line between air and the MORB endmember as defined by Sarda et al. (1988), i.e., $^{20}Ne/^{22}Ne = 13$, $^{21}Ne/^{22}Ne = 0.07$. The difference between the two samples is due to different degrees of air contamination. The three surface gas samples

Table 2. Gas samples from Laacher See and Wallenborn

Sample No.	Date	^4He [ppm]	$^3He/^4He$ [10^{-6}]	^{20}Ne [ppb]	$^{20}Ne/^{22}Ne$	$^{21}Ne/^{22}Ne$ [10^{-2}]	^{40}Ar [ppm]	$^{40}Ar/^{36}Ar$	$C/^3He$ [10^9]
Laacher See, Position LA4, taken in shallow water from the surface									
169	31.5.91	17.0 (3)	7.264 (35)	26.1 (6)	9.786 (34)	2.859 (35)	–[a]	–[a]	8.1[b]
174	31.5.91	19.8 (4)	7.239 (35)	61.6 (13)	9.749 (64)	2.835 (39)	–[a]	–[a]	7.0[c]
249	2.9.93	17.3 (4)	7.234 (56)	19.6 (5)	9.95 (13)	2.881 (66)	–[a]	–[a]	8.0[c]
Laacher See, Position LA2, taken by divers in 31 m depth									
245	2.9.93	11.9 (2)	7.327 (58)	3.87 (10)	9.915 (27)	2.974 (19)	43.8 (45)	391 (4)	11.5[c]
Well "Wallenborn", Wallenborn, West Eifel									
30	1.6.91	52.3 (11)	3.691 (19)	1.61 (4)	11.21 (6)	4.87 (5)	–[a]	–[a]	5.2[d]
68	3.9.93	55.7 (12)	3.670 (28)	7.08 (17)	10.19 (3)	3.430 (39)	29.8 (30)	1060 (4)	4.9[e]
Atmospheric values for comparison[f]									
-	-	5.24	1.384	16'450	9.80	2.90	9300	295.5	0.04

Errors (one standard deviation) are quoted in parentheses referring to the last digits.
[a] Not determined
[b] Measured CO_2 content: 99.7 %
[c] calculated assuming same CO_2 content as in [b].
[d] Measured CO_2 content: >99.9 %
[e] calculated assuming same CO_2 content as in [d].
[f] Values for dry air, taken from OZIMA and PODOSEK (1983), except $^3He/^4He$ according to CLARKE et al. (1976).

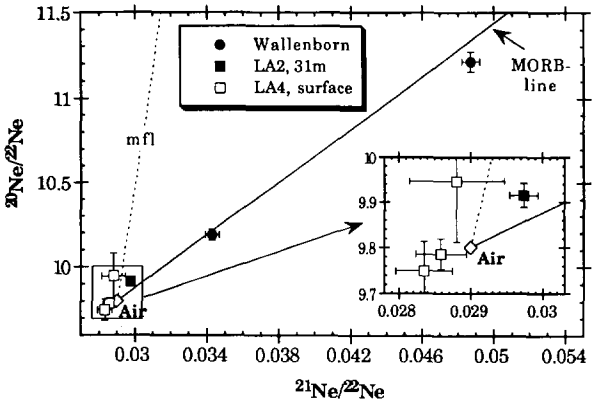

FIG. 5. Three-isotope diagram of neon, showing data of gas samples from Laacher See and the well "Wallenborn" (see Table 2). The samples from Laacher See lie close to the point representing the neon composition of air (see enlarged insert). Only the sample collected by divers at LA2 at 31 m depth significantly differs from air (1σ errors shown, see discussion in text). The samples from Wallenborn seem to follow the indicated mixing trend between the atmosphere and a MORB endmember as definded by Sarda et al. (1988). The mass fractionation line (mfl) indicates the trend produced by isotope fractionation of air neon.

from Laacher See (position LA4) plot close to the air point but appear slightly shifted to the left. However, for none of the three points and not even for their average, the difference in $^{21}Ne/^{22}Ne$ from the air value is significant on the 2σ level (1σ errors shown in Fig. 5). Even if this shift would be real (e.g., due to an experimental offset, although we have no indication for that) the following discussion would not be affected. In contrast to the samples from LA4, the sample collected by divers at LA2 is different from air on the 2σ-level, but not from the air-MORB line.

The fact that the samples from Wallenborn and LA2 follow an air-MORB mixing line is rather surprising, because—as discussed before—the $^3He/^4He$ ratios are below the MORB value and indicate significant contributions from crustal radiogenic helium, especially in Wallenborn. Since nucleogenic neon (mainly ^{21}Ne) is produced in fairly constant proportions to radiogenic helium (Kennedy et al., 1990), crustal neon would shift the points in Fig. 5 to the right.

An attempt for a consistent interpretation of the isotopic signatures of helium and neon in the samples from the Eifel has been made by Kipfer et al. (1994b). The neon data have been corrected for nucleogenic neon, based on measured $^3He/^4He$ ratios and $^{21}Ne/^4He$ production ratios from the literature. Similar calculations were performed by Honda et al. (1993) to demonstrate that the initial isotopic composition of noble gases in the Earth was of solar origin. Although our data from the Eifel do not perfectly match the model of Honda et al. (1993), they neither contradict it provided that the uncertainties of the model parameters are considered. Yet, a thorough discussion of the neon isotopes in the mantle is beyond the scope of this paper.

4.3. Quantification of the Helium Flux into Laacher See

The simplest way to quantify the helium flux into Laacher See is by calculating the change of the lake's total helium content between the two sampling dates (31 May and 4 September). Provided it can be assumed that the helium concentrations at a given depth are constant across the lake, the helium content can be calculated by weighting the values measured at the central position (LA1) with the depth-dependent cross-sectional area of the lake, taken from Scharf and Menn (1992). The following total changes are calculated: $(8.8 \pm 0.3)\cdot 10^6$ cm^3 STP for ^4He and (66 ± 2) cm^3 STP for ^3He. Divided by the total lake area of 3.31 km^2 and the time interval of 96 days, this results in a specific flux of $(8.6 \pm 0.3)\cdot 10^{12}$ atoms m^{-2} s^{-1} for ^4He and $(6.4 \pm 0.2)\cdot 10^7$ atoms m^{-2} s^{-1} for ^3He.

Since in the above calculation any loss of injected helium from the lake is neglected, these values must be lower limits to the true fluxes. As the temperature profiles (Fig. 2) show, only the hypolimnion below about 15 m depth remained fairly undisturbed during the summer. Only gas that is dissolved in the hypolimnion is efficiently trapped in the lake, whereas the gas injected at shallower depth can partially escape to the atmosphere. Therefore, a better estimate of the helium flux should result by restricting the mass balance to the hypolimnion below 15 m depth. This layer covers 80% of the lake's surface and 60% of its volume, but contains 90% of the helium increment. Hence, the revised calculation yields specific fluxes which are about 10% larger, i.e., $(9.6 \pm 0.3)\cdot 10^{12}$ atoms m^{-2} s^{-1} for ^4He and $(7.1 \pm 0.2)\cdot 10^7$ atoms m^{-2} s^{-1} for ^3He.

So far, a uniform distribution of the flux over the entire sediment area was assumed. However, the shape of the helium profile determined in September 1991 (Fig. 3a) shows that this assumption is not correct. Apparently, local helium sources exist at depths between 20 and 30 m, but not in the deepest part of the lake. As a further attempt, a budget calculation is made only for the layer below 30 m (60% of the lake's surface, 25% of its volume, 40% of the helium increment). The following specific fluxes are calculated: $5.7\cdot 10^{12}$ atoms m^{-2} s^{-1} for ^4He and $4.2\cdot 10^7$ atoms m^{-2} s^{-1} for ^3He. This is about 60% of the flux calculated from the total hypolimnion budget. Thus, 40% of the helium flux must originate from the point sources.

There still remain a few shortcomings in the above calculations. First, as shown by Fig. 3a, the helium concentration is not really constant at a fixed depth. The few available data from noncentral positions (see Figs. 1 and 3) show a clear maximum near position LA2 and a weak minimum at LA3. The size of typical horizontal concentration differences can be estimated by using coefficients of horizontal eddy diffusivity, K_h, measured in several Swiss lakes of similar size to lie within the range of 0.02 to 0.3 m^2 s^{-1} (Peeters, 1994). In Laacher See, typical horizontal distances from the central position, L_h, at 30 m depth and deeper are about 500 m. The time needed to overcome L_h by horizontal diffusion is given by $t = L_h^2/2K_h = 5$ to 70 days. In the most extreme case horizontal inhomogeneities could "hide" the helium input of up to a few weeks. A value of a few days is probably more realistic, since as long as horizontal mixing is at steady state the change of the helium content is less influenced by horizontal inhomogeneities than the absolute values. The error of the flux calculations due to unknown horizontal helium distribution is estimated to be ±20%, at most.

A second source of uncertainty is the direct escape of gas bubbles to the atmosphere. Based on the reports of the divers who sampled the gas plume at position LA2 we think that most of the gas is dissolved in the lake and only a small fraction escapes.

A third problem relates to the loss of helium through the thermocline by turbulent diffusion. The coefficient of vertical turbulent diffusion, K_z, can be determined from the temperature data (Fig. 2) by applying the standard budget-gradient method described by Powell and Jassby (1974). This yields K_z values in the range of $(1 \text{ to } 5) \cdot 10^{-6}$ m^2 s^{-1}, except for higher values near the surface and the bottom. At 15 m depth the vertical diffusivity is $1.5 \cdot 10^{-6}$ m^2 s^{-1}. Such values are typical for thermoclines in lakes (e.g., Imboden et al., 1983). The time-averaged vertical ^{3}He concentration gradient at this depth is $-1.7 \cdot 10^{12}$ atoms m^{-4} (z positive upwards). The flux per unit total lake area (A_0) through the thermocline (area A_{th}) can be calculated from the first Fickian law:

$$F = -\frac{A_{th}}{A_0} K_z \cdot \frac{\partial C}{\partial z} .$$

This yields an upwards flux of ^{3}He of $2.0 \cdot 10^6$ atoms m^{-2} s^{-1}. Since this is only about 3% of the total flux as estimated before, the correction due to turbulent diffusion is not important.

It may become necessary to use more advanced tools to calculate helium fluxes into lakes. As an example, we mention the one-dimensional vertical model CHEMSEE that was developed in our group (Johnson et al., 1991; Ulrich, 1991). CHEMSEE is a user-friendly simulation software package that provides the general structure of a one-dimensional lake model and includes lake-specific information, e.g., lake topography, coefficients of vertical diffusion, and the velocity of gas exchange at the surface. The relevant processes can be chosen according to the physical and chemical properties of the variable (e.g., ^{3}He) to be modeled.

The version of CHEMSEE that is appropriate for helium in Laacher See includes vertical K_z-profiles derived from the water temperature and a value for the gas exchange velocity (e.g., 1 m d^{-1}, see Imboden et al., 1981). Different assumptions for the helium flux have been tested according to their ability to predict the helium profiles of September 1991, starting from the profiles measured in May. Figure 6 shows the results of two different model runs. In model H (homogeneous), a uniform sediment flux of $7.1 \cdot 10^7$ ^{3}He atoms m^{-2} s^{-1} is assumed as determined from the hypolimnion budget approach. This model cannot reproduce the concentration maximum at 25 m depth. In model P (point source), the flux is split into a uniform contribution (60% of the total flux) and a depth dependent point source (40% of the total flux). As it turns out, the best agreement between the measurements and the model is reached if the point source is evenly spread between 18 and 28 m depth. The lower boundary of this range agrees with the observation of the divers that the bubbles are dissolved within a few meters above the point of gas injection. The upper boundary might be related to the diffusive barrier provided by the thermocline.

To summarize, the best estimate for the ^{4}He flux into Laacher See is $(10 \pm 2) \cdot 10^{12}$ atoms m^{-2} s^{-1} with a ^{3}He/^{4}He-ratio of $(7.42 \pm 0.03) \cdot 10^{-6}$. This value may still be a lower limit since helium may be lost in bubbles escaping to the atmosphere. 60% of the flux is rather homogeneously distributed over the sediment area, the remaining 40% arise from the gas injections near the eastern shore at depths between 20 and 30 m. In summer, the hypolimnion retains the incoming helium almost completely, only 3% is lost by vertical mixing. During the circulation of the water body in winter, however, the considerable quantities of gases, in particular CO_2, that are stored in the lake must be released to the atmosphere.

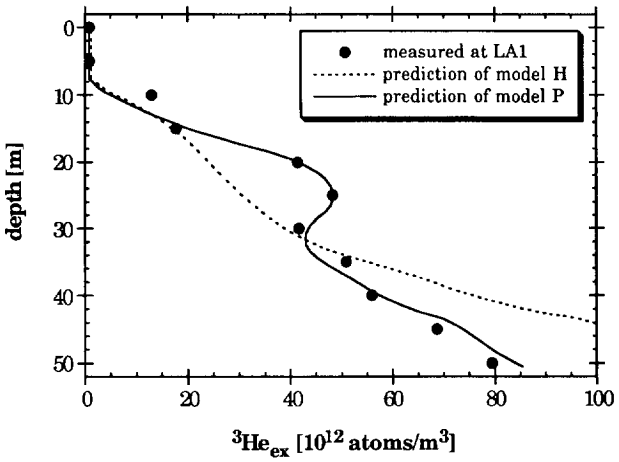

FIG. 6. Prediction of the ^{3}He excess profile measured in September 91 at position LA1, calculated with a one-dimensional vertical lake model (CHEMSEE). For Model H (homogeneous flux) a uniform flux of mantle-derived ^{3}He of $(7.1 \pm 0.2) \cdot 10^7$ atoms m^{-2} s^{-1} is assumed. The model cannot reproduce the concentration maximum at 25 m depth. A better fit is obtained by Model P (point source) for which a local input of helium in the layer between 18 and 28 m is introduced that contributes 40% of the total helium flux.

4.4. Fluxes of Other Species

The main gas injected into Laacher See is CO_2, while noble gases are present in trace amounts only. If it were possible to determine constant ratios between ^{3}He and other gases, then the fluxes of these gases could be calculated. Yet, as mentioned before, in the water samples from the lake no mantle derived noble gas other than helium can be identified. However, the gas samples with very little air contamination can serve to establish isotopic ratios between the mantle contributions of the different species.

4.4.1. CO_2

Although CO_2 was measured in two samples only (Table 2, No. 169 and 30), it is reasonable to assume that all gas samples consist of nearly pure CO_2 (see also the data by Giggenbach et al., 1991). Therefore, atomic C/^{3}He ratios can be readily calculated. In our gas samples from Laacher See they vary between 7.0 and $11.5 \cdot 10^9$ (Table 2). Giggenbach et al. (1991) found values between 3 and $5 \cdot 10^9$, whereas Griesshaber et al. (1992) reported a very high ratio of $280 \cdot 10^9$ for one gas sample from Laacher See. These results demonstrate the difficulties with the C/^{3}He relationship which prevent a separation of the CO_2 at Laacher See into contributions from the mantle and the crust. The carbon-helium systematics of

Table 3. Helium fluxes, C/^{3}He and heat/^{3}He ratios in lakes

Lake (country)	Area [km^2]	^{4}He flux $\cdot 10^{-12}$ [atoms m^{-2} s^{-1}]	^{3}He/^{4}He [10^{-6}]	C/^{3}He [10^9]	heat/^{3}He [10^{-9} J/atom]	Reference
Laacher See (Germany)	3.31	10 ± 2	7.42 ± 0.03	8.6 ± 1.0	1.0 ± 0.2	this study
Lake Nyos (Cameroon)	1.49	300 ± 40	7.84 ± 0.04	30 ± 15	0.29 ± 0.04	SANO et al., 1990
Lake Mashu (Japan)	20	0.92	9.43 ± 0.17	180	170	IGARASHI et al., 1992
Crater Lake (USA)	53	0.55	9.9	40	100	COLLIER et al., 1991
Lake Nemrut (Turkey)	11	≥ 6	10.32 ± 0.06	37 ± 22 [a]	12 ± 1	KIPFER et al., 1994a

[a] Unpublished data: average of three gas samples from the Nemrut Caldera that were not discussed by KIPFER et al., 1994a.

the Eifel is discussed in detail by Griesshaber et al. (1992). We base the following rough estimate of the CO_2 flux into Laacher See on the average C/^{3}He-ratio of our own gas samples from the lake, i.e., $(8.6 \pm 1.0)\cdot 10^9$. Combining this value with the ^{3}He flux of $(7.4 \pm 1.5)\cdot 10^7$ atoms m^{-2} s^{-1}, we get a CO_2 flux of $(6.4 \pm 1.5)\cdot 10^{17}$ molecules m^{-2} s^{-1} or 33 ± 8 mol m^{-2} y^{-1}. The total amount of CO_2 released from the lake in one year is $(1.1 \pm 0.3)\cdot 10^8$ mol or about 5000 tons.

The yearly turnover of CO_2 at Laacher See is orders of magnitude less than the amount of CO_2 that was instantaneously released during the catastrophe at Lake Nyos in 1986; the estimates range between $2.4\cdot 10^5$ tons (Giggenbach, 1990) and $2.4\cdot 10^6$ tons (Kling et al., 1987). Since degassing of Laacher See occurs rather regularly in every winter, hazardous accumulation of CO_2 in Laacher See seems unlikely.

4.4.2. *Neon and argon*

The following calculations are based on the results from the gas sample No. 245 taken by divers at position LA2 (Table 2). It is the only sample from the lake in which non-atmospheric neon and argon could be measured. In order to estimate the flux of these noble gases from the mantle, the measured concentrations have to be split into contributions from the mantle and atmosphere, respectively. This can be done by using the measured isotopic ratios of ^{20}Ne/^{22}Ne and ^{40}Ar/^{36}Ar, provided that these ratios are known for the two endmember reservoirs, atmosphere and mantle.

For neon, the atmospheric ratio $(^{20}Ne/^{22}Ne)_a$ is 9.80 (Table 2), and the mantle ratio $(^{20}Ne/^{22}Ne)_{man}$ presumably lies in the range between the solar wind value of 13.8 (Benkert et al., 1993) and the MORB value of 13 estimated by Sarda et al. (1988). The corresponding range of the mantle contribution of ^{20}Ne to sample No. 245 from Laacher See is 4.0 to 4.7%. Thus, the mixing calculation is rather insensitive to the exact value of $(^{20}Ne/^{22}Ne)_{man}$. In view of the above discussion of the neon results from Wallenborn, we adopt the solar wind value for further calculations.

The corresponding decomposition is speculative for argon, since its evolution in the mantle is subject of controversial discussions (see Dunai and Baur, 1995; Fisher, 1994; Staudacher et al., 1989). Recently, it was even speculated that there might be no juvenile ^{36}Ar left in the depleted mantle (Fisher, 1994). Yet the presence of more mobile juvenile noble gases, such as ^{3}He and ^{20}Ne, in the Eifel region suggest that some juvenile ^{36}Ar should be left, as well. Thus, to derive a rather conservative estimate of the mantle flux of argon we adopt a mantle argon ratio $(^{40}Ar/^{36}Ar)_{man} \geq 35000$, i.e., the largest value ever observed in fluid inclusions of MORB samples (Fisher, 1994). Using the atmospheric ratio of 295.5 (Table 2) and the value measured in sample No. 245 of 391 ± 4 yields a mantle contribution of 0.28% for ^{36}Ar. Using for the $(^{40}Ar/^{36}Ar)_{man}$ ratio the lower MORB value given by Staudacher et al. (1989) would increase this value to 0.34%.

Combined with the absolute concentrations given in Table 2 and assuming that all ^{3}He is derived from the mantle, the following atomic ratios are calculated for the mantle component:

$$(^{20}Ne/^{3}He)_{man} = 1.8 \pm 0.3$$

$$(^{36}Ar/^{3}He)_{man} \leq 3.5 \pm 0.6.$$

The uncertainties include all experimental errors and the uncertainty that originates from the unknown composition of the mantle component.

The deduced elemental noble gas ratios lie between the values calculated from Staudacher et al. (1989) for the upper and lower mantle, respectively. To summarize, our best estimates of the mantle derived fluxes into Laacher See are

^{3}He-flux: $(7.4 \pm 1.5)\cdot 10^7$ atoms m^{-2} s^{-1},

^{20}Ne-flux: $(13 \pm 4)\cdot 10^7$ atoms m^{-2} s^{-1},

^{36}Ar-flux: $\leq (26 \pm 7)\cdot 10^7$ atoms m^{-2} s^{-1}.

The corresponding total radiogenic fluxes are

^{4}He-flux: $(10 \pm 2)\cdot 10^{12}$ atoms m^{-2} s^{-1},

^{40}Ar-flux: $\leq (9.2 \pm 2.5)\cdot 10^{12}$ atoms m^{-2} s^{-1}.

4.4.3. *Heat*

In deep stratified lakes the geothermal heat flow can often be estimated from the temperature gradient close to the bottom. Sometimes, as in Lake Nemrut, Turkey (Kipfer et al., 1994a) or in Lake Nyos (Sano et al., 1990), the gradients of helium concentration and temperature are linearly related and give directly a heat/^{3}He ratio. Yet, the temperature structure in Laacher See is dominated by diffusive transport from the surface rather than from the bottom. Therefore, heat flow cannot be quantified from water temperatures. However, using the heat flow of 76 mW m^{-2} determined from temperature gradients in the sediments (Haenel, 1983) yields a heat/^{3}He-ratio of $1.0\cdot 10^{-9}$ J/atom. This is much less than values measured in hydrothermal springs in the ocean (e.g., Baker and Lupton, 1990; Lupton et al., 1989; Jenkins et al., 1978).

Table 3 summarizes the few existing data on the heat/^{3}He ratio measured in lakes of volcanic origin. Two of them, Lake Nyos and Laacher See, both the product of continental CO_2 based volcanism, have a rather small heat/^{3}He flux ratio. They

seem to indicate an increasing flux ratio with age (Lake Nyos is 400 years old, Kling et al., 1987; Laacher See about 11000 years, Bogaard and Schmincke, 1985), but with only two studies generalization of this finding must remain speculative.

In contrast, lakes that are related to subduction volcanism (Lake Mashu, Igarashi et al., 1992; and Crater Lake, Collier et al., 1991) have heat/^{3}He ratios that are much larger and closer to the values found in the submarine hydrothermal systems of the ocean (Baker and Lupton, 1990; Lupton et al., 1989; Jenkins et al., 1978). Lake Nemrut, located at the continental triple junction of the European, Afro-Arabian, and the Persian plate, occupies a middle position between the two extremes (Kipfer et al., 1994a). Further studies, especially on other maar lakes, will show whether the relationship between age and heat/^{3}He flux ratio is generally valid and thus may lead to a better understanding of the transport of energy and fluids through the continental crust.

5. CONCLUSIONS

To our knowledge, this is the first report on helium fluxes into lakes that includes isotopic anomalies and flux estimates of other noble gases. Such data can help to understand origin and driving forces behind these gas fluxes. Lakes bear a great potential to study mantle volatile fluxes in active continental areas. We expect that considerable helium fluxes with isotopic signature of the mantle also exist in many other volcanic lakes, e.g., Lake Monoun in Cameroon (Giggenbach et al., 1991) or Lac Pavin in France from which we have preliminary data. Similar helium results were also found in the submarine Sakurajima Caldera, Kagoshima Bay, in Japan (Craig and Horibe, 1994).

A shortcoming of the hitherto published studies on helium fluxes in lakes consists in a lack of proper understanding of the physics in the particular lakes. Thus, most of the flux calculations listed in Table 3 are rough estimates only because most of the studies neglect the vertical flux of dissolved gases by turbulent diffusion during the stratification period.

The helium fluxes determined in volcanic lakes are far greater than the average flux into the ocean, e.g., $7.4 \cdot 10^7$ ^{3}He atoms m^{-2} s^{-1} in Laacher See compared to the mean oceanic flux of $4 \cdot 10^4$ ^{3}He atoms m^{-2} s^{-1} (Craig et al., 1975). Yet, due to the restricted area of these lacustrine sources their overall contribution to the global helium flux is small (e.g., in the order of 10^{-5} for Laacher See). All continental mantle helium sources combined would probably not change the present global helium flux estimates very much. However, the study of volatile fluxes, as well as isotopic and elemental ratios in waters and gases of rather small natural "collection pans," may significantly contribute to the understanding of the mechanisms behind the Earth's degassing processes.

Acknowledgments—We gratefully acknowledge the friendly support by Burkhard Scharf, Martina Oehms, and co-workers from the Landesamt für Wasserwirtschaft, Rheinland Pfalz, in Mainz, Germany. Important background information on the Eifel was provided by Tibor Dunai who joined the first expedition. Roland Hohmann took part on the third expedition and helped in the laboratory. Special thanks go to the divers on the third expedition, Bettina Rinne and Adrian Kaiser, who collected a very important sample under the most difficult conditions. U. Ott, E. Griesshaber, F. Stuart, and T. Torgersen are acknowledged for their comments and constructive reviews.

Editorial handling: U. Ott

REFERENCES

Aeschbach-Hertig W. (1994) Helium and Tritium als Tracer für physikalische Prozesse in Seen. Ph.D. dissertation No. 10714, ETH Zürich.

Bahrig B. (1985) Sedimentation und Diagenese im Laacher Seebecken (Osteifel). Ph.D. dissertation, Institut für Geologie der Ruhr-Universität Bochum.

Baker E. T. and Lupton J. E. (1990) Changes in submarine hydrothermal ^{3}He/heat ratios as an indicator of magmatic/tectonic activity. *Nature* **346,** 556–558.

Baur H. (1980) Numerische Simulation und praktische Erprobung einer rotationssymmetrischen Ionenquelle für Gasmassenspektrometer. Ph.D. dissertation No. 6596, ETH Zürich.

Benkert J.-P., Baur H., Signer P., and Wieler R. (1993) He, Ne, and Ar from the solar wind and solar energetic particles in lunar ilmenites and pyroxenes. *J. Geophys. Res.* **98,** 13,147–13,162.

Benson B. B. and Krause D. (1980) Isotopic fractionation of helium during solution: A probe for the liquid state. *J. Soln. Chem.* **9,** 895–909.

Bogaard P. and Schmincke H.-U. (1985) Laacher See Tephra: A widespread isochronous late Quaternary tephra layer in central and northern Europe. *GSA Bull.* **96,** 1554–1571.

Clarke W. B., Beg M. A., and Craig H. (1969) Excess ^{3}He in the sea: Evidence for terrestrial primordial helium. *Earth Planet. Sci. Lett.* **6,** 213–220.

Clarke W. B., Jenkins W. J., and Top Z. (1976) Determination of tritium by mass spectrometric measurement of ^{3}He. *Intl. J. Appl. Radiat. Isotopes* **27,** 515–522.

Collier R. W., Dymond J., and McManus J. (1991) Studies of hydrothermal processes in Crater Lake, OR. Report No. 90-7, College of Oceanography, Oregon State Univ.

Craig H. and Horibe Y. (1994) ^{3}He and methane in Sakurajima Caldera, Kagoshima Bay, Japan. *Earth Planet. Sci. Lett.* **123,** 221–226.

Craig H., Clarke W. B., and Beg M. A. (1975) Excess ^{3}He in deep water on the East Pacific Rise. *Earth Planet. Sci. Lett.* **26,** 125–132.

Dunai T. J. and Baur H. (1995) Helium, neon, and argon systematics of the European subcontinental mantle: Implications for its geochemical evolution. *Geochim. Cosmochim. Acta* **59,** 2767–2783.

Fisher D. E. (1994) Mantle and atmospheric-like argon in vesicles of MORB glasses. *Earth Planet. Sci. Lett.* **123,** 199–204.

Fuchs G., Roether W., and Schlosser P. (1987) Excess ^{3}He in the ocean surface layer. *J. Geophys. Res.* **92,** 6559–6568.

Giggenbach W. F. (1990) Water and gas chemistry of Lake Nyos and its bearing on the eruptive process. *J. Volcanol. Geotherm. Res.* **42,** 337–362.

Giggenbach W. F., Sano Y., and Schmincke H. U. (1991) CO_2-rich gases from Lakes Nyos and Monoun, Cameroon; Laacher See, Germany; Dieng, Indonesia, and Mt. Gambier, Australia—variations on a common theme. *J. Volcanol. Geotherm. Res.* **45,** 311–323.

Griesshaber E., O'Nions R. K., and Oxburgh E. R. (1992) Helium and carbon isotope systematics in crustal fluids from the Eifel, the Rhine Graben and Black Forest, F.R.G. *Chem. Geol.* **99,** 213–235.

Haenel R. (1983) Geothermal investigations in the Rhenish Massif. In *Plateau Uplift The Rhenish Shield—A case history* (ed. K. Fuchs et al.), pp. 228–246. Springer.

Honda M., McDougall I., Patterson D. B., Doulgeris A., and Clague D. A. (1993) Noble gases in submarine pillow basalts glasses from Loihi and Kilauea, Hawaii: A solar component in the Earth. *Geochim. Cosmochim. Acta* **57,** 859–874.

Igarashi G., Ozima M., Ishibashi J., Gamo T., Sakai H., Nojiri Y., and Kawai T. (1992) Mantle helium flux from the bottom of Lake Mashu, Japan. *Earth Planet. Sci. Lett.* **108,** 11–18.

Imboden D. M., Lemmin U., Joller T., Fischer K. H., and Weiss W. (1981) Lake mixing and trophic state. *Verh. Internat. Verein. Limnol.* **21,** 115–119.

Imboden D. M., Lemmin U., Joller T., and Schurter M. (1983) Mixing processes in lakes: Mechanisms and ecological relevance. *Schweiz. Z. Hydrol.* **45,** 11–44.

Jenkins W. J., Edmond J. M., and Corliss J. B. (1978) Excess ^{3}He and ^{4}He in Galapagos submarine hydrothermal waters. *Nature* **272,** 156–158.

Johnson C. A., Ulrich M., Sigg L., and Imboden D. M. (1991) A mathematical model of the manganese cycle in a seasonally anoxic lake. *Limnol. Oceanogr.* **36,** 1415–1426.

Kennedy B. M., Reynolds J. H., and Smith S. P. (1988) Noble gas geochemistry in thermal springs. *Geochim. Cosmochim. Acta* **52,** 1919–1928.

Kennedy B. M., Hiyagon H., and Reynolds J. H. (1990) Crustal neon: a striking uniformity. *Earth Planet. Sci. Lett.* **98,** 277–286.

Kipfer R. (1991) Primordiale Edelgase als Tracer für Fluide aus dem Erdmantel. Ph.D. dissertation No. 9463, ETH Zürich.

Kipfer R., Aeschbach-Hertig W., Baur H., Hofer M., Imboden D. M., and Signer P. (1994a) Injection of mantle type helium into Lake Van (Turkey): The clue for quantifying deep water renewal. *Earth Planet. Sci. Lett.* **125,** 357–370.

Kipfer R. et al. (1994b) Neon degassing of the subcontinental mantle under the Eifel region, Germany. *Abstracts of ICOG-8, USGS Circular 1107,* 172.

Kling G. W. et al. (1987) The 1986 Lake Nyos gas disaster in Cameroon, West Africa. *Science* **236,** 169–175.

Lippolt H. J. (1983) Distribution of volcanic activity in space and time. In *Plateau Uplift The Rhenish Shield—A case history* (ed. K. Fuchs et al.), pp. 112–120. Springer.

Lorenz V. (1973) On the formation of maars. *Bull. Volcanol.* **37,** 183–204.

Lupton J. E. (1983) Terrestrial inert gases: Isotope tracer studies and clues to primordial components in the mantle. *Ann. Rev. Earth Planet. Sci.* **11,** 371–414.

Lupton J. E., Baker E. T., and Massoth G. J. (1989) Variable ^{3}He/heat ratios in submarine hydrothermal systems: evidence from two plumes over the Juan de Fuca ridge. *Nature* **337,** 161–164.

Oxburgh E. R., O'Nions R. K., and Hill R. I. (1986) Helium isotopes in sedimentary basins. *Nature* **324,** 632–635.

Ozima M. and Podosek F. A. (1983) *Noble Gas Geochemistry.* Cambridge Univ. Press.

Peeters F. (1994) Horizontale Mischung in Seen. Ph.D. dissertation No. 10476, ETH Zürich.

Polve M. and Kurz M. D. (1984) Helium isotopic and fission track studies of ultramafic xenoliths. *Eos* **65,** 697.

Powell T. and Jassby A. (1974) The estimation of vertical eddy diffusivities below the thermocline in lakes. *Water Resour. Res.* **10,** 191–198.

Puchelt H. (1982) Kinetische Kohlenstoff-Isotopenfraktionierung im CO_2-H_2O-System des Laacher Sees. *Ber. Bunsenges. Phys. Chem.* **86,** 1041–1043.

Sano Y. et al. (1990) Helium and carbon fluxes in Lake Nyos, Cameroon: Constraint on next gas burst. *Earth Planet. Sci. Lett.* **99,** 303–314.

Sarda P., Staudacher T., and Allègre C. J. (1988) Neon isotopes in submarine basalts. *Earth Planet. Sci. Lett.* **91,** 73–88.

Scharf B. W. and Menn U. (1992) Hydrology and morphometry. *Arch. Hydrobiol. Beih. Ergebn. Limnol.* **38,** 43–62.

Scharf B. W. and Oehms M. (1992) Physical and chemical characteristics. *Arch. Hydrobiol. Beih. Ergebn. Limnol.* **38,** 63–83.

Schmidt-Ries H. (1955) Zur Physiographie der Eifelmaare. *Gewäss. Abwäss.* **9/10,** 7–112.

Staudacher T., Sarda P., Richardson S. H., Allègre C. J., Sagna I., and Dmitriev L. V. (1989) Noble gases in basalt glasses from a Mid-Atlantic Ridge topographic high at 14°N: geodynamic consequences. *Earth Planet. Sci. Lett.* **96,** 119–133.

Stute M., Sonntag C., Déak J., and Schlosser P. (1992) Helium in deep circulating groundwater in the Great Hungarian Plain: Flow dynamics and crustal and mantle helium fluxes. *Geochim. Cosmochim. Acta* **56,** 2051–2067.

Torgersen T. and Clarke W. B. (1987) Helium accumulation in groundwater, III. Limits on helium transfer across the mantle-crust boundary beneath Australia and the magnitude of mantle degassing. *Earth Planet. Sci. Lett.* **84,** 345–355.

Torgersen T., Top Z., Clarke W. B., Jenkins W. J., and Broecker W. S. (1977) A new method for physical limnology—tritium-helium-3 ages—results for Lakes Erie, Huron and Ontario. *Limnol. Oceanogr.* **22,** 181–193.

Ulrich J. (1958) Die Mineralquellen der Vulkaneifel und ihre wirtschaftliche Auswertung. *Gewäss. Abwäss.* **19,** 66–80.

Ulrich M. (1991) Modeling of chemicals in lakes—development and application of user-friendly simulation software (MASAS and CHEMSEE) on personal computers. Ph.D. dissertation No. 9632, ETH Zürich.

Weiss R. F. (1971) Solubility of helium and neon in water and seawater. *J. Chem. Eng. Data* **16,** 235–241.

Welhan J. A. and Craig H. (1983) Methane, hydrogen and helium in hydrothermal fluids at 21°N on the East Pacific Rise. In *Hydrothermal Processes at Seafloor Spreading Centers* (ed. P. A. Rona et al.), pp. 391–409. Plenum Press.

Wüest A., Brooks N. H., and Imboden D. M. (1992) Bubble Plume Modeling for Lake Restoration. *Water Resour. Res.* **28,** 3235–3250.